On the Evolution of Phase Patterns during the High-Impact-Modified Polystyrene Process

M. Fischer[†] and G. P. Hellmann*[,‡]

Deutsches Kunststoff-Institut, Schlossgartenstrasse 6, D-64289 Darmstadt, Germany

Received June 5, 1995; Revised Manuscript Received October 25, 1995[⊗]

ABSTRACT: High-impact-modified polystyrene (HIPS) is made by thermal or radical polymerization of styrene containing dissolved polybutadiene (PB). The reaction leads, intermediately, to blends of yet ungrafted PB, of the homopolymer PS, and of graft copolymers PBgS varying in the number of PS grafts per PB chain. The polymerization induces a phase separation and a phase inversion which results in the well-known "salami" morphology of HIPS. To elucidate the mechanism producing this morphology, the polymerization of styrene in PB/styrene mixtures was studied kinetically and morphologically, in toluene solution and in the bulk. Besides the conventional techniques of polymerization kinetics, electron microscopy was employed to examine the PS/PB/PBgS blends that are formed during the polymerization. The electron micrographs reflect sensitively the composition of these blends, the architecture of the PBgS graft copolymers, and the miscibility of PBgS with PS and PB. The blends were isolated from the polymerizing system by two methods, i.e. (i) evaporation of styrene and (ii) dissolution and film casting. Method i preserves the in-situ morphology of the polymerizing system, while method ii leads to a thermodynamically controlled morphology. Pairwise comparison of these two types of morphology reveals that HIPS owes its salami structures to the fact that PBgS chains with two grafts or more can solubilize the homopolymer PS while PBgS chains with only one graft cannot.

1. Introduction

For four decades now, high-impact polystyrene (HIPS) has been a standard thermoplastic. Yet, the peculiar process of HIPS production, via the polymerization of styrene containing dissolved polybutadiene (PB),[1−4] is still intriguing. HIPS is basically a blend of polystyrene (PS) and a graft copolymer of butadiene and styrene (PBgS) that displays characteristic phase morphologies, as shown in Figure 1:[5,6] Substructured "salami" phase domains of the graft copolymer PBgS are embedded in a matrix of PS. The domains are not purely elastomeric but are heavily filled with PS subdomains. The PB forms in fact only thin lamellar microphases (black in Figure 1), on the outside of the domains and on the inside, between the subdomains. HIPS owes its superior impact strength to these elastomeric microphases.[7−9]

The salami domains in Figure 1 are quite anomalous for blends:[6,10−18] Figure 2a shows the domain-matrix morphology of a PS/PB homopolymer blend. The elastomeric domains are simple spheres of neat PB, without a substructure. Substructures inside phase domains can be introduced by block[6,12−15] or graft[16−18] copolymers. Figure 2b shows a PS/PSbBbS blend with triblock copolymer PSbBbS where the copolymer forms domains that exhibit a lamellar microstructure. However, this substructure looks completely different from that in Figure 1. This obvious difference between the salami domains of HIPS and other blend structures is discussed below.

HIPS is a product by process, whose morphology results from the in-situ character of the grafting reaction and from the process technology.[1−6] The original solution of PB in styrene turns, as the styrene is polymerized, intermediately into a *styrene solution of PS/PB/PBgS ternary blends* varying in composition. The main features of the peculiar domain structure of Figure 1 are created in fairly early stages of the polymerization.[5,6]

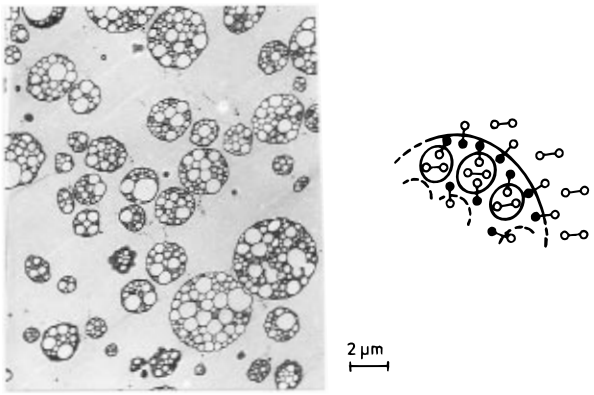

Figure 1. Salami structures in commercial HIPS (from BASF AG), made of PS (○−○) and the graft copolymer PBgS (●−○) (In all electron micrographs of this paper: (black) butadiene, (white) styrene phases.)

This study was carried out to elucidate details of the HIPS process. The kinetics of the styrene polymerization in PB/styrene mixtures were studied with conventional techniques as well as with electron microscopy, in dilute toluene solution and in the bulk.

The PS/PB/PBgS blends were extracted from the polymerizing system (i) via precipitation and film casting or (ii) via direct styrene evaporation (in the bulk runs). Method i leads to thermodynamically controlled morphologies while method ii preserves the in-situ morphologies of the polymerizing system. The advantage of cast films is that they display thermodynamically favored morphologies that are easier to interpret than the in-situ morphologies.

2. HIPS

Industrially made HIPS results from thermal or peroxide-initiated styrene polymerization in mixtures with PB, at PB:styrene weight ratios on the order of 1:10. The "salami" morphology in Figure 1 is controlled by three factors that are discussed for the peroxide-initiated process:

* To whom all mail should be sent.
[†] Present address: BASF AG, D-67056 Ludwigshafen, Germany.
[‡] In memory of Prof. Dr. Dr. h.c. Heinrich Hellmann, a lifelong passionate chemist.
[⊗] Abstract published in *Advance ACS Abstracts,* December 15, 1995.

0024-9297/96/2229-2498$12.00/0

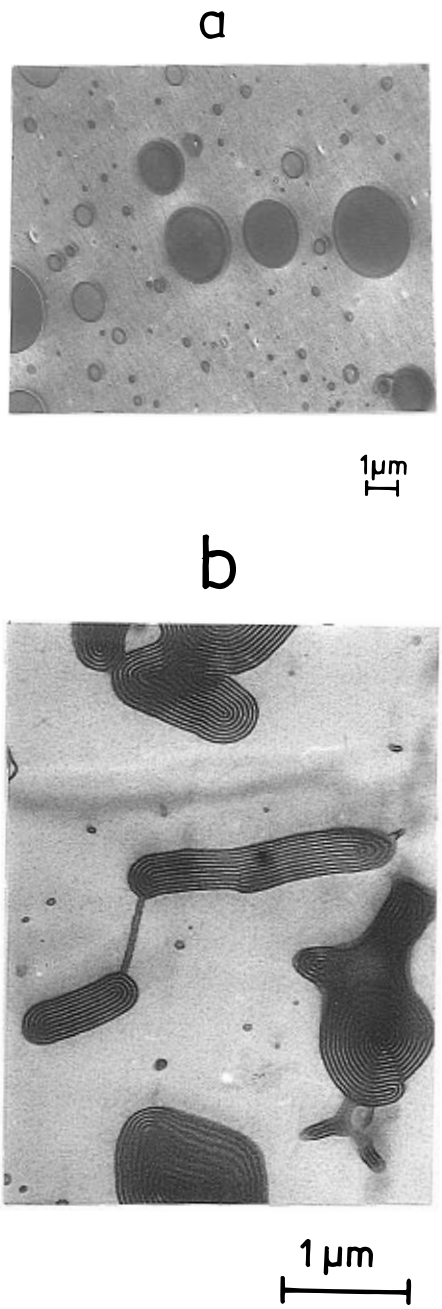

Figure 2. Domain-matrix morphology of (a) a PS/PB homopolymer blend and (b) a PS/PSbBbS blend with a triblock copolymer. (Polymers from BASF AG: PS, 168N, molecular weight $M_w = 330 \times 10^3$; PSbBbS, molecular weight overall 105 $\times$ 10^3, monodisperse. Molecular weights of the blocks are nearly equal.)

(i) Homopolymerization and Graft Copolymerization (Figure 3a).[1−4,19,20] Peroxide initiators (RO−OR) attack not only the styrene monomers (S) but also the PB chains. The initiator radicals abstract allylic hydrogen atoms or add to the double bonds of the 1,4- and 1,2-butadiene units.[16] The competition of homopolymerization and graft copolymerization is parameterized, in Figure 3a, by the selectivity of the initiator radicals

$$C = (k_{PB}/k_S)/(M_B/M_S) \qquad (1)$$

k_i = rate constants;

M_i = monomer molecular weights

The grafting converts the PB chains successively into

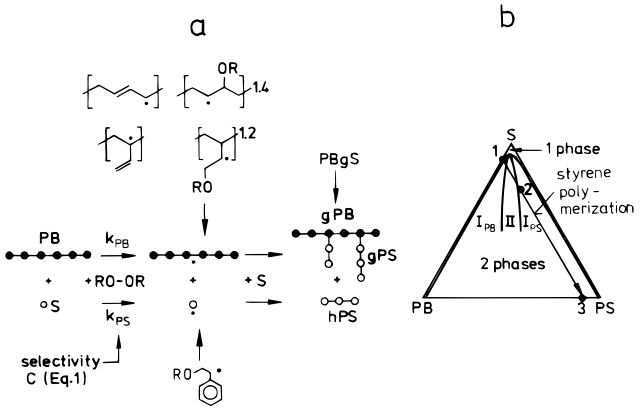

Figure 3. (a) Polymerization in a PB/styrene (PB/S) mixture with a peroxide RO−OR, yielding homopolymer (hPS) and graft copolymer (PBgS) chains (chain symbols: circles filled for PB and empty for PS). (b) Phase triangle of PS/PB/styrene blend solutions. Miscibility gap (two phases) with sectors of cocontinuous (II) and domain-matrix morphologies (matrix PS (I_{PS}) or PB (I_{PB})). Styrene polymerization is indicated by the arrow 1 → 2 → 3.

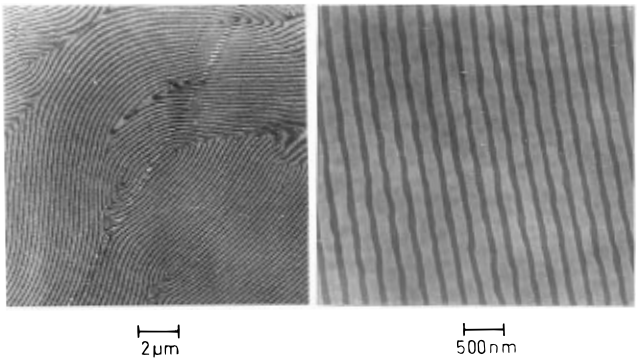

Figure 4. Lamellar microphase morphology of a graft copolymer PBgS (extracted product of the rapidly stirred bulk polymerization, section 5.2).

copolymer chains PBgS. At high styrene conversions, the majority of the PB chains contain at least one graft: The original PB/styrene mixture is converted approximately into a binary PS/PBgS polymer blend, as indicated in Figure 1. In between, the system is quaternary, i.e. PS/PB/PBgS/styrene.

(ii) Phase Separation (Figure 3b).[1−4,21−23] The styrene polymerization provokes a phase separation, because PS and PB are incompatible. It is easier to envisage the situation without grafting (which can be suppressed by using azo initiators).[19] Figure 3b shows the phase diagram of PS/PB/styrene blend solutions. Polymerization is indicated by an arrow starting from a PB/styrene mixture ("1"). The system enters, at a very low styrene conversion, a miscibility gap where a new phase, PS/styrene, segregates from the PB/styrene matrix phase (sector I_{PB}).[21−23] The new phase collects all PS being generated in both phases and grows, inducing a phase inversion, still at a fairly low conversion: After a transition stage with cocontinuous phase structures (sector II), the PS/styrene phase takes over the matrix ("2", sector I_{PS}). This happens at approximately equal volumes of PS and PB. At total conversion ("3"), finally, a PS/PB blend is formed with macrophase domains of PB that are dispersed in PS, as shown in Figure 2a.

The phase separation and the matrix inversion I_{PB} → II → I_{PS} occur similarly during the polymerization of HIPS where grafting takes place, by which the PB is

transformed successively into the copolymer PBgS. But the morphology of the final PS/PBgS blend is different, because the graft copolymer PBgS itself is a microheterogeneous system. Its chains consist of incompatible gPB and gPS subchains that demix, intramolecularly. Pure PBgS copolymers build structures of separate microphases on the scale of chain coil diameters, as shown in Figure 4. Therefore, in blends with homopolymers, these copolymers must lead to complex macrophase−microphase morphologies.[24−26] However, simple mixing leads either to structures as in Figure 2b or to micelles of the copolymer, but never to the unique salami structures of Figure 1.

(iii) Stirring and Cross-Linking. The industrial polymerization process for HIPS is divided into two steps, as indicated in Figure 3b. Step 1 → 2 is carried out at lower and step 2 → 3 at higher temperatures.

Crucial for the morphology of the PS/PBgS blend is step 1 → 2, where grafting and phase inversion control the macrophase−microphase balance of the final morphology. This balance is sensitive to the stirring conditions.[24−26] Stirring does not change micelles but perturbs lamellar microphases (Figure 4) and disperses macrophases (Figure 2). In step 2 → 3, the styrene is polymerized to completion, at slow stirring, predominantly by homopolymerization. The phase structure does not change anymore. It is stabilized by the high viscosity of the matrix and finally fixed by cross-linking in the elastomeric gPB domains. The final PS/PBgS blend, i.e. the HIPS, has a stable morphology (Figure 1) that survives further processing unaltered.

In summary, the morphology of HIPS is controlled by effects due to (i) the chemistry, (ii) the physics, and (iii) the technology of the polymerization process. To exclude the problems associated with points ii and iii, the following study deals first with the polymerization of styrene in dilute homogeneous PB/styrene/toluene solutions. Then, this situation is compared to polymerization in the bulk, i.e. in undiluted PB/styrene mixtures. The bulk polymerization simulates the HIPS process.

3. Theory

The system in Figure 3a consists, once the reactions are underway, of the homopolymers hPS and hPB and the graft copolymer PBgS with its gPB subchains and gPS grafts (disregarding styrene and the solvent). The following model predictions concern grafting in the homogeneous state, i.e. in solution. The composition of the hPS/hPB/PBgS ternary blends obtained by precipitating the polymers at different times of the polymerization is characterized. The equations are commented on in the Appendix.

Initially, the system consists of PB and styrene in the ratio

$$R = m_S(t=0)/m_{PB} \qquad m_i = \text{mass (in all equations)} \tag{2}$$

Polymerization of the styrene, described by the conversion

$$\pi(t) = m_{PS}(t)/m_{PB} = R(1 - e^{-kt}) \qquad k = \text{rate constant} \tag{3}$$

leads to hPS homopolymer chains and gPS copolymer grafts, in a ratio controlled by the initiator selectivity C (eq 1, Figure 3a). For fairly nonselective initiators, the fraction of the homopolymer hPS depends barely on the conversion π (unless $\pi \rightarrow R$):

$$f_{hPS} = m_{hPS}/m_{PS} \cong R/(R + C) \tag{4}$$

The molecular weights (throughout, number averages are considered) of hPS and gPS are approximately equal. They, too, do not depend markedly on π (unless $\pi \rightarrow R$):

$$M_{hPS} \cong M_{gPS} \cong M_{PS} \qquad M_i = \text{molecular weight} \tag{5}$$

While hPS is statistically decoupled from hPB and PBgS, hPB and PBgS are coupled. The copolymer PBgS is actually a series of copolymers carrying more or less grafts, and the homopolymer hPB is, in this series, the member with no grafts. Since longer PB chains are grafted statistically more frequently, the hPB chains are at $\pi > 0$ always shorter and the gPB subchains longer than the chains of the original PB.

The architecture of the graft copolymer PBgS depends on the molecular weights of the original PB and of the gPS grafts, M_{PB} and M_{PS}, and on the polymerization parameters π and f_{hPS}. The number of grafts G per PBgS chain is

$$G(\pi) = (m_{gPS}/m_{gPB})/(M_{gPS}/M_{gPB}) \cong 1 + G^*(\pi) \tag{6}$$

where

$$G^*(\pi) = (m_{gPS}/m_{PB})/(M_{PS}/M_{gPB}) = (1 - f_{hPS})\pi(M_{PB}/M_{PS}) \tag{7}$$

is the number of grafts if the ungrafted homopolymer hPB and the graft copolymer PBgS are averaged together (G and G^* are number averages).

Other parameters can be expressed as functions of G. The fraction of the homopolymer hPB is given by

$$f_{hPB}(\pi) = (m_{hPB}/m_{PB})(\pi) \cong 1/G(\pi)^2 \tag{8}$$

and its molecular weight is given by

$$M_{hPB}(\pi) = M_{PB}/G(\pi) \tag{9}$$

Both f_{hPB} and M_{hPB} drop with π. The graft copolymer PBgS is characterized by the set (M_{gPB}, G, M_{gPS}), where

$$M_{gPB}(\pi) \cong M_{PB}(1 + G(\pi))/G(\pi) \tag{10}$$

while G and M_{gPS} are given by eqs 6 and 5. The combined molecular weight of PBgS is

$$M_{PBgS}(\pi) \cong M_{gPB}(\pi) + G(\pi)M_{PS} \tag{11}$$

A known oddity of grafting is that this total molecular weight M_{PgS} grows usually much less than linearly with $G(\pi)$.[27] It can even decrease, since $M_{gPB}(\pi)$ in eq 11 is decreasing with π, due to the fact that the longest PB chains are grafted first, because they are statistically preferred.

The distribution of components in the hPS/hPB/PBgS blend is described by the weight fractions w_i of the polymers

$$w_{hPS}(\pi) = (m_{hPS}/m)(\pi) = f_{hPS}\pi/(1 + \pi)$$

$$w_{hPB}(\pi) = (m_{hPB}/m)(\pi) = f_{hPB}(\pi)/(1 + \pi)$$

$$w_{PBgS}(\pi) = 1 - (w_{hPS} + w_{hPB})(\pi) \tag{12}$$

The composition x (weight fraction of gPS) of the graft

copolymer PBgS, to be written more precisely in the form $PB_{1-x}gS_x$, is given by

$$x(\pi) = (m_{gPS}/m_{PBgS})(\pi) = \pi/((1 - f_{hPB}(\pi))/(1 - f_{hPS}) - \pi) \quad (13)$$

The above equations describe the kinetics in a homogeneous solution. In demixed systems, the kinetics are naturally more complex, but it will be seen below that, nonetheless, the processes can be quite similar in the homogeneous and the demixed state.

4. Experimental Section

Polybutadiene (Aldrich) with the monomer units 1,4-cis (40), 1,4-trans (45), and 1,2 (15 mol %), molecular weights of $M_w = 290 \times 10^3$ and $M_w/M_n = 2.2$, and a glass transition temperature of $T_g = -86$ °C was used.

The styrene polymerizations in solution (PB/styrene/toluene) and in the bulk (PB/styrene) were carried out in simple two-neck glass flasks, filled to one-third, using a glass blade (100 rpm) or a metal propeller stirrer (1500 rpm, only in the bulk). PB was dissolved in styrene and toluene (solution runs) or only in styrene (bulk runs). The concentrations, i.e. the ratio R of styrene and PB (eq 2) and, in the solution runs, the total weight fraction of PB/styrene in toluene, are specified below. Styrene was polymerized at 70 °C, using 1.7 mmol/mol (with reference to styrene) of the radical initiator dibenzoyl peroxide.

Samples were taken at different times of polymerization. The hPS/hPB/PBgS blends were isolated by two methods: (i) The samples were precipitated in methanol, sometimes after dilution with toluene, the blends were redissolved in toluene, and films were cast (100 μm thick) from the toluene solutions (2% w/w, slow casting at room temperature over 1 day, under a gentle, indirectly guided stream of nitrogen). (ii) The samples (only from bulk runs) were dried directly.

In both cases, the samples were heated in the final stages of drying, but never markedly above the (rising) glass transition temperature. Therefore, the structures were not changed by annealing effects, during the drying.

To isolate the pure graft copolymer PBgS, the homopolymer hPS was extracted with 2-butanone/acetone (3:2 v/v) and the homopolymer hPB with petroleum benzene. The blends and polymers were characterized by GPC (PS calibration), IR spectroscopy, and DSC. Ultrathin sections were cut from the samples, contrasted with OsO_4, and examined under the transmission electron microscope.

Samples with much PB were hardened by pretreatment with OsO_4 and were sometimes cut at cryotemperatures. In the pictures, PB phases are dark and PS phases are light. Contrast variations in the pictures are due to slight variations in the preparations of samples and photographs.

5. Results

One representative polymerization run in dilute solution is described first (Figures 5−11). It was analyzed kinetically in detail. The model equations quoted above could be applied because the solutions remained homogeneous throughout the reaction. The results are then compared with polymerization runs in the bulk.

5.1. Grafting in Solution. In the ratio $R = 6$ (eq 2, corresponding to 17% w/w of PB), styrene and PB were dissolved in toluene, the concentration of PB/styrene being, in toto, 4% w/w.

Blend and Copolymer Composition. The styrene conversion $\pi(t)$, measured gravimetrically after precipitation of the hPS/hPB/PBgS blends, is shown in Figure 5a, with a fit of eq 3. The polymerization was stopped at $\pi = 2.5$. To show that this amounts to less than half the total styrene conversion, the limit $\pi(t\rightarrow\infty) = R$ is indicated in Figure 5a. The solutions remained always

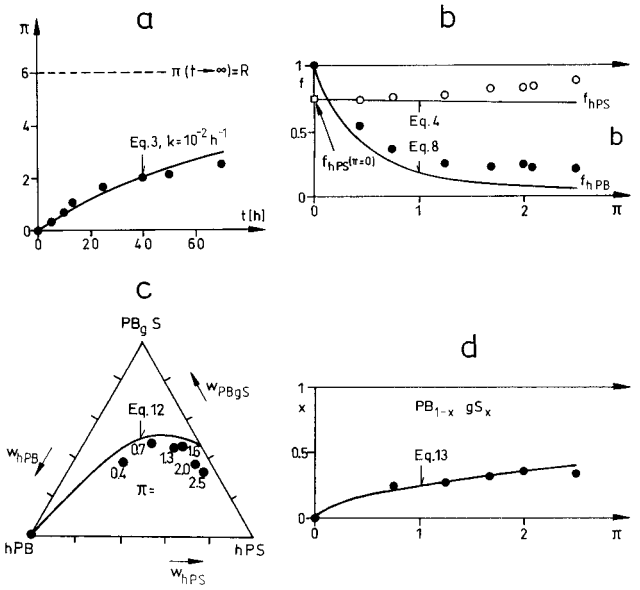

Figure 5. Polymerization kinetics in dilute homogeneous solution: (a) conversion $\pi(t)$ and (b) homopolymer fractions $f_{hPS}(\pi)$ and $f_{hPB}(\pi)$, (c) composition of the hPS/hPB/PBgS blends as a function of the conversion π (w_i: weight fractions), (d) composition $x(\pi)$ (weight fraction of styrene) of the graft copolymer $PB_{1-x}gS_x$.

clear, and precipitated blends could always be redissolved completely.

Figure 5b shows the homopolymer fractions f_{hPS} and f_{hPB}, determined after extraction, as functions of π. Both homopolymers are formed in excess of the predictions of eqs 4 and 8. The fraction f_{hPB} seems to approach an asymptote, $f_{hPB}(\pi\rightarrow R) \cong 0.2$, meaning that always a residue of ungrafted PB remains.

The intercept $f_{hPS}(\pi\rightarrow 0) = 0.75$ in Figure 5b yields, with eq 4 (which is exact at $\pi \rightarrow 0$), the initiator selectivity $C \cong 2$ (Figure 3a): The rate constants of graft copolymer and homopolymer formation are thus of the same order (eq 1). In ref 19, a lower value is reported for C, the homopolymerization being slightly favored. In any case, dibenzoyl peroxide is quite a nonselective initiator in this reaction system.

The compositions of the hPS/hPB/PBgS blends are shown in Figure 5c. Compared to the curve calculated with eq 12, the copolymer content is a bit low. Blends with a maximum content of the copolymer PBgS are obtained near the conversion $\pi = 1$, where the total of polymerized styrene, hPS + gPS, equals the total of PB, hPB + gPB.

Figure 5d shows the weight content x of styrene in the graft copolymer $PB_{1-x}gS_x$, with a fit of eq 13. At all conversions that were considered, the copolymer PBgS contains more butadiene than styrene.

Molecular Weights. The GPC curve in Figure 6a of the hPS/hPB/PBgS blend that was precipitated at $\pi = 2.5$ shows two peaks, one each on either side of the peak of the original PB that is characterized by $M_w = 290 \times 10^3$ ($M_n = 130 \times 10^3$).

Fractionation by extraction revealed the substructure of the complex peak in Figure 6a. The separate contributions of the extracted homopolymers hPS and hPB and of the copolymer PBgS are shown in Figure 6b. The figure reveals that the low molecular weight peak in Figure 6a belongs to the homopolymer hPS. Total destruction of the gPB subchains of the copolymer PBgS with OsO_4 yielded almost the same peak, which confirms eq 5: The hPS chains and the gPS grafts are of

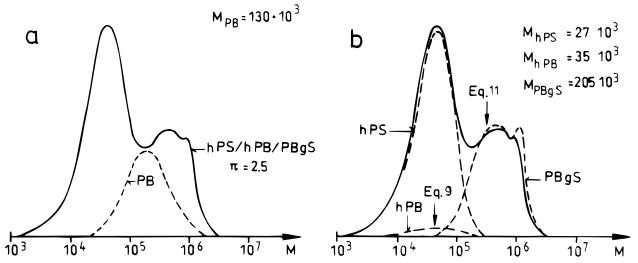

Figure 6. (a) GPC curves of the original homopolymer PB and the hPS/hPB/PBgS blend obtained at the conversion $\pi = 2.5$. (b) Separate GPC curves of the components hPS, hPB, and PBgS of the blend, measured after extraction. M_i: number average molecular weights. The arrows indicate the model predictions.

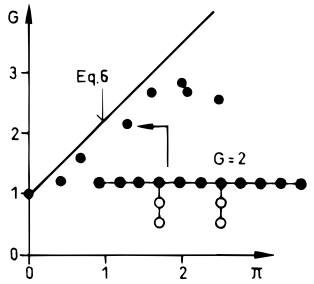

Figure 7. Number average number of grafts $G(\pi)$ of the copolymer PBgS, a graft copolymer with two grafts being indicated.

practically equal lengths, the molecular weight being $M_w = 60 \times 10^3$ ($M_n = 27 \times 10^3$).

The copolymer PBgS consists thus of short gPS grafts on a long gPB main chain. A tiny peak in Figure 6b belongs to the remaining ungrafted homopolymer hPB. As predicted by eq 9, its chains are, at $M_w = 75 \times 10^3$ ($M_n = 35 \times 10^3$), much shorter than those of the original PB. At this fairly high conversion ($\pi = 2.5$), all longer PB chains are already grafted.

The number of grafts G, calculated with eqs 7 and 6, is shown in Figure 7. To visualize the type of architecture produced at high conversions π, a graft copolymer PBgS with $G = 2$ is indicated, schematically. Compared to the model prediction of eq 6, G is low at higher π, which reflects the high f_{hPS} in Figure 5b.

The GPC curve of the graft copolymer PBgS in Figure 6b seems bimodal. However, the upper peak, in the range of millions, is an artifact. The curve should decay steadily and end in a tail, but the GPC columns fail at these high molecular weights.

Regardless if peak or tail, there are certainly products with molecular weights in the millions which are not predicted by simple grafting kinetics. They must be due to microgels, most probably formed via radical combination of grafts. The copolymer PBgS was fractionated once more, this time by precipitation. The longest-chained fractions contained less styrene, according to elemental analysis: The microgels seem to contain, besides PBgS, also some ungrafted hPB.

In summary, the polymerization reactions follow basically straightforward kinetics, with some minor deviations that disfavor grafting and introduce some microgels. The copolymer PBgS obtained at $\pi = 2.5$ is approximately characterized by the parameter set

$$M_{gPB} \cong 180\ 000,\ G = 2.5,\ M_{gPS} = 27\ 000$$

where G and M_{gPS} were measured directly (Figures 7 and 6b) and M_{gPB} was calculated with eq 10.

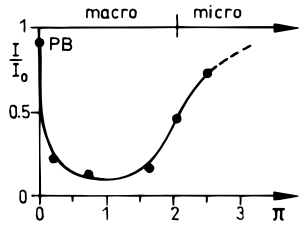

Figure 8. Light transmission I/I_o of the hPS/hPB/PBgS blends as a function of π.

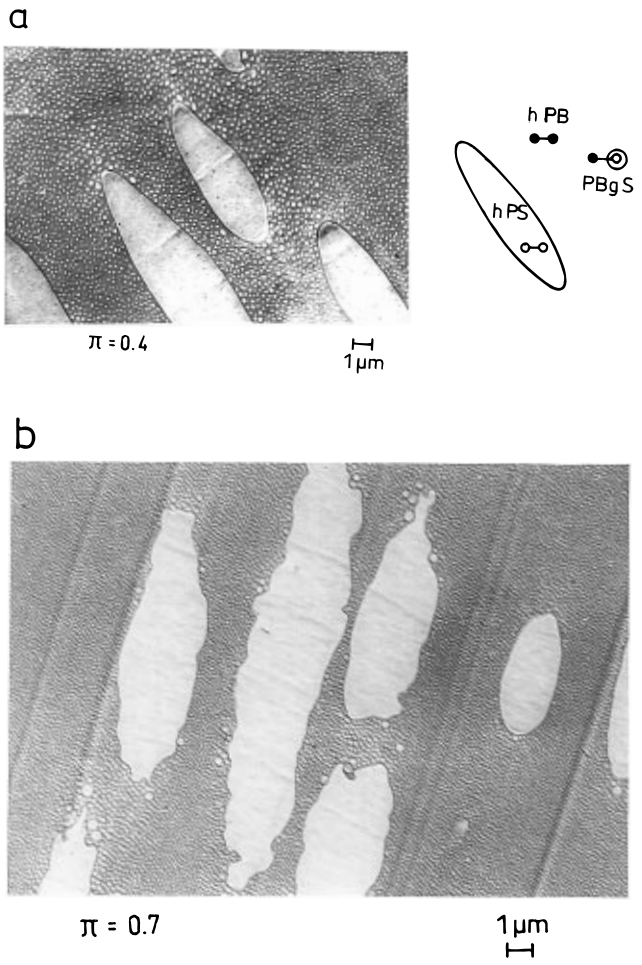

Figure 9. Macrophases of hPS in a matrix of hPB that is filled with micelles of PBgS(G=1), at low conversions: (a) $\pi = 0.4$, (b) $\pi = 0.7$. In (a), the components hPB (●–●), hPS (○–○), and PBgS (●–○) are indicated.

Blend Morphologies. hPS/hPB/PBgS blends were isolated from the polymerizing solution at different π by precipitation, redissolution and film casting. The blend films were examined turbidimetrically and by transmission electron microscopy. The question was whether the homopolymers hPS and hPB would form separate macrophases or whether the graft copolymer PBgS would turn these macrophases into microstructures.

Figure 8 shows the transmission of light. The film of the original PB ($\pi = 0$) was transparent. But the films of the blends formed at $\pi > 0$ were mostly opaque. Only at high conversions, at $\pi > 2$, did the blend films clear up again.

Correspondingly, the electron micrographs of the hPS/hPB/PBgS blends in Figures 9 and 10 show a transition from macrophase to microphase separation, caused by the ongoing grafting. [The phase domains in Figures 9

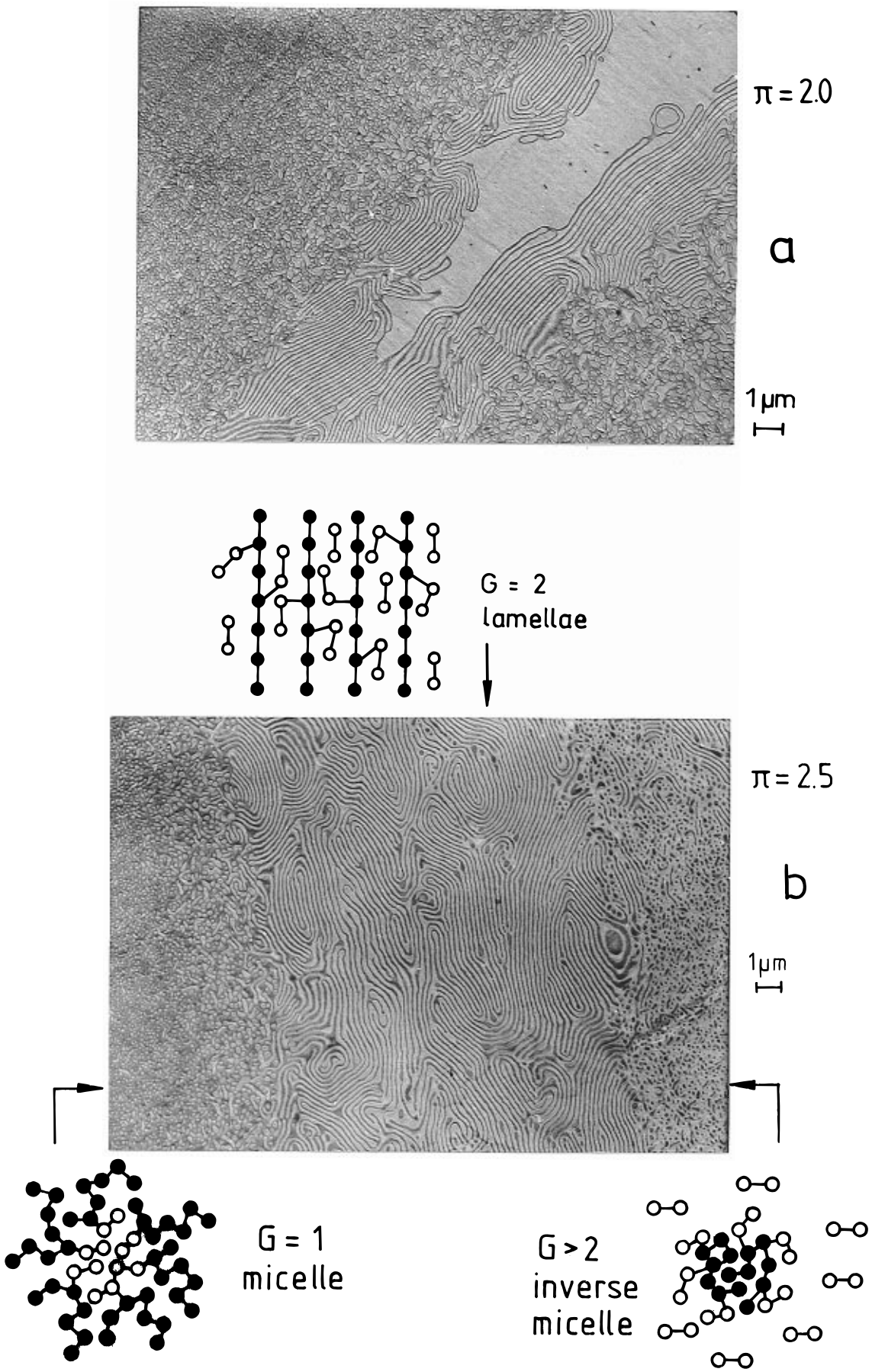

Figure 10. (a) Macrophase of hPS, surrounded by a multilayer of copolymer chains PBgS(G=2), in a hPB/PBgS(G=1) matrix, close to the macrophase−microphase transition, at the conversion $\pi = 2.0$. (b) Micellar, inverse-micellar, and lamellar structures of copolymer chains PBgS differing in the number of grafts G ($G = 1, 2, >2$), after the macrophase−microphase transition, at the conversion $\pi = 2.5$.

and 10 are elongated, i.e. oriented. This will be disregarded. Films that are prepared by solvent evaporation from originally very dilute solutions often display oriented morphologies.]

As shown in Figures 9 and 10a, the blends develop macrophase morphologies up to $\pi = 2$. At very low π, in Figure 9a, the homopolymer hPS forms macrodomains on the scale of micrometers, while the copolymer PBgS forms much smaller micelles that float in the matrix of hPB. At higher π, the situation changes gradually in characteristic stages. The ternary blend in Figure 9b appears already binary, i.e. as a hPS/PBgS blend. The homopolymer hPB still present is barely seen. The macrodomains of hPS have now an irregular shape. In Figure 10a, at $\pi = 2$, the macrodomains of hPS are surrounded by lamellar microphases of PBgS. This indicates the transition to microphase morphologies.

There are no remaining macrophases of hPS in Figure 10b. All hPS is dispersed in the microphase structure of PBgS. Nonetheless, the morphology is not homogeneous. The figure shows three phases: On the left, there is a micellar phase reminiscent of the matrix phase in Figure 10a. In the center, there is a phase with a lamellar structure, as observed around the macrodomain of hPS in Figure 10a. On the right in Figure 10b, there is an inverse-micellar phase, with hPS in the role of the matrix. This phase is not observed at lower conversions.

As indicated in Figure 10b, the micellar phases feature spherical and cylindrical (on the left) or inverse-spherical and inverse-cylindrical (on the right) micelles of PBgS.

A straightforward interpretation of Figure 10b is that the three phases are due to an internal fractionation of the graft copolymer PBgS with respect to the number of grafts G. In fact, all electron micrographs in Figures 9 and 10 permit a distinction of PBgS copolymer chains with one, two, or more grafts. The classification is indicated in Figure 10b.

G = 1. The copolymers forming micelles in the left-hand phase in Figure 10b and also inside the matrix in all pictures of Figures 14−16 carry only *one graft*. At low π, all copolymer chains are of this type, i.e. PBgS(G=1). Figure 9a reveals clearly the properties of these chains. They form micelles with a core of gPS grafts and a corona of gPB backbones. The corona is not seen, because it mixes intimately with the matrix of hPB. These micelles of PBgS(G=1) do not solubilize the homopolymer hPS, which forms, therefore, macrodomains of its own. The macrodomains in Figure 9a do not contain any graft copolymer micelles, and their smooth surface indicates that they are not covered by graft copolymer chains. All this proves that the PBgS(G=1) copolymer chains are practically unable to mix with hPS.

G = 2. The copolymers forming lamellae in the center phase of Figure 10b and surrounding the macrodomain in Figure 10a in a multilayer carry *two grafts*. Figure 10b proves that these copolymers PBgS(G=2) solubilize both hPB and hPS: There are no macrophases of the homopolymers anymore; in other words, the copolymer chains "compatibilize" the system. This is a bit surprising, because the copolymers PBgS(G=2) are compositionally by no means symmetric. They consist of much more gPB than gPS (formula in Figure 7). At lower π, in Figure 9b, no lamellar microphases are seen, but the copolymers PBgS(G=2) are apparently already present in minor amounts. They cover the surface of the macrodomains of hPS in Figure 9b, lowering the interfacial tension. The domains are, therefore, irregularly shaped, as opposed to the domains in Figure 9a which have a smooth surface.

G > 2. The copolymers in the right-hand phase in Figure 10b carry *more than two grafts*. They form inverse micelles, with the PB backbones in the core and the gPS grafts in the corona. These micelles float in a matrix of hPS.

The distinction between $G = 2$ and $G > 2$ is only based on Figure 10b and may not be considered absolutely certain. Much more important is the distinction between $G = 1$ and $G \geq 2$ that is reflected by all pictures of Figures 9 and 10 and can be considered proven beyond a doubt. Below, it will turn out to be the key for an understanding of the salami structures of HIPS.

The picture conveyed so far is that "graft copolymer chains with $G = 1$ cannot but chains with $G \geq 2$ can solubilize hPS". Two notes are added to moderate this a bit.

(i) One cannot precisely distinguish between the two classes $G = 1$ and $G > 1$. A PBgS chain carrying one long graft should behave like a chain with two short grafts, and a chain with a particularly long gPB backbone, carrying two grafts, should behave like a chain with a short backbone and only one graft.

(ii) One cannot say strictly that the PBgS(G=1) copolymer chains do not solubilize hPS. Some micelles in Figure 9a are too large, and the matrix phase in Figure 9b is clearly swollen with hPS. Yet, the copolymer PBgS(G=1) is unable to solubilize the macrodomains of hPS. Consequently, one assumes that this indicates a further fractionation effect: PBgS(G=1) can solubilize short chains of hPS, but not the long chains which separate off in the macrodomains.

In summary, Figures 9 and 10 demonstrate that the cast-film morphologies at different conversions π reflect sensitively the composition of the hPS/hPB/PBgS blends and the architecture of the graft copolymer chains. Fractionation effects and the ability of the PBgS(G) copolymer chains to mix more or less with the homopolymers hPS and hPB are directly seen.

There is some inconsistency between Figure 7 and the pictures in Figures 9 and 10, concerning the number of grafts G per PBgS chain. Looking at the micrographs, it seems that the values of G in Figure 7 are a bit high at $\pi < 2$ and too constant at $\pi > 2$. The pictures in Figures 9 and 10 give the impression of a steadily increasing number of grafts $G(\pi)$ that reaches $G = 2$ not before $\pi = 2$ and keeps increasing at $\pi > 2$. Of course, the electron micrographs cannot be evaluated quantitatively.

Graft Copolymer Microstructures. Looking at the three phases in Figure 10b, one should suspect that the PBgS copolymer chains differing in the number of grafts G, formed in the same reaction, are immiscible. But the electron micrographs in Figure 11 of the pure copolymers PBgS, after extraction of the homopolymers, prove differently. All figures display homogeneous microstructures of the copolymer PBgS, without separate phases. Figure 11a features spherical micelles, as in the corresponding Figure 9a. More interesting are the pictures in Figure 11b,c. They correspond to Figure 10a,b where copolymers from $G = 1$ to $G > 2$ were separated into different phases. No such fractionation is observed in Figure 11b,c. Each extracted copolymer

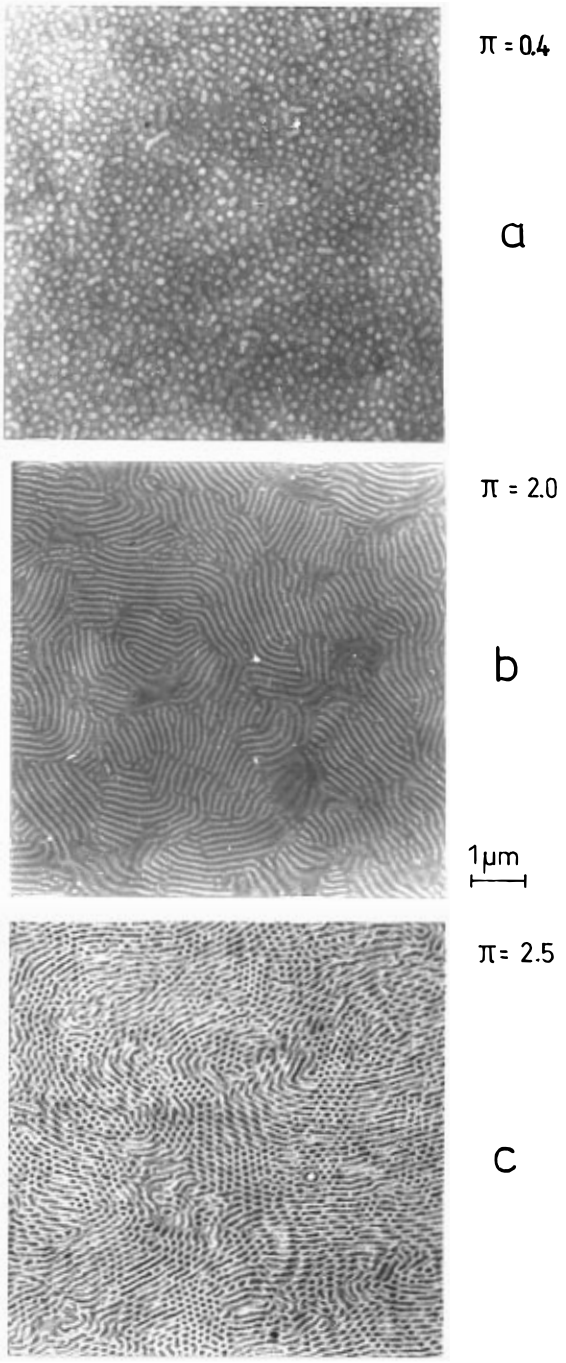

Figure 11. Graft copolymers PBgS extracted at increasing conversion π: (a) micelles, (b) lamellae, (c) inverse micelles.

PBgS forms one microstructure only. It is lamellar ($G = 2$ behavior) in Figure 11b, at $\pi = 2.0$, and inverse-cylindrical ($G > 2$ behavior) in Figure 11c, at $\pi = 2.5$.

Consequently, the fractionation of copolymer chains differing in the number of grafts G must be brought about by the homopolymers hPS and hPB. This is not surprising. Polymers are extremely selective, as far as mixing partners are concerned, and thus extremely efficient fractionation agents.

The type of microstructure in Figure 11c deserves attention: At the conversion $\pi = 2.5$, the copolymer PBgS has approximately three gPS grafts (Figure 7). But these grafts, together, have only half the molecular weight of the gPB backbone ($x \cong {}^1/_3$, Figure 5d). Nonetheless, this copolymer forms inverse-cylindrical micelles: The long gPB backbones fill the center of the cylinders while the gPS grafts point outward. This is a consequence of the "barbed wire" architecture of graft copolymers.

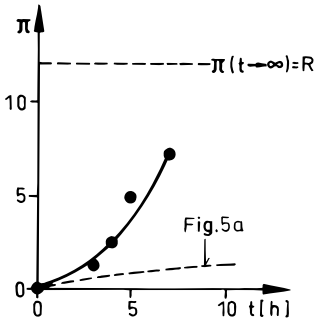

Figure 12. Conversion $\pi(t)$ of the styrene polymerization in a rapidly stirred PB/styrene mixture, in the bulk, compared to $\pi(t)$ in solution (Figure 5a).

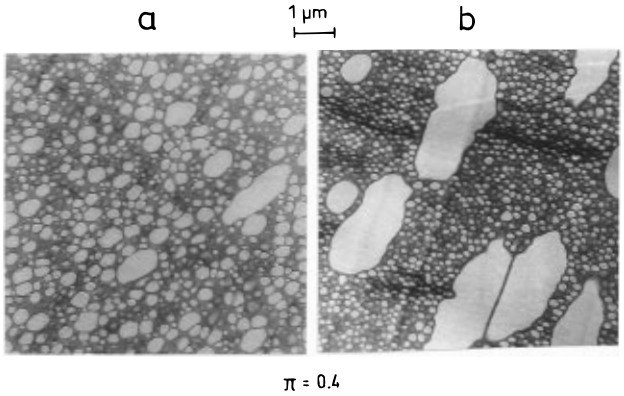

Figure 13. Bulk polymerization, fast stirring: (a) in situ and (b) cast-film morphology at low conversion ($\pi = 0.4$) (matrix: PB).

5.2. Grafting in the Bulk. The PB/styrene system described so far was homogeneous only due to high dilution with toluene. Polymerization in less dilute toluene solutions and in the bulk PB/styrene system itself led, in situ, to phase separation.

A solution twice as concentrated as the one discussed in the previous section demixed during polymerization. In the undiluted bulk system, demixing started already at a few percent of conversion.[21−23]

Two bulk runs will be discussed. They are characterized below in Figures 12−16. Styrene and PB were mixed in the ratio $R = 12$ (eq 2, corresponding to 8% w/w of PB). A lower PB concentration than in solution was employed in the bulk runs, in order to keep the viscosity down. Due to the higher concentrations in the bulk and the gel effect, the styrene polymerized faster than in solution (Figure 12), despite the phase separation.

Slow Stirring. In a first bulk run, the stirring was done as in the solution runs, i.e. with a glass blade stirrer, at 100 rpm. The phase separation and slow stirring, together, are known to inhibit grafting,[24−26] and the grafting efficiency was indeed very low. The morphology had no microstructure. A fairly coarse cocontinuous morphology was observed, built up by the two homopolymers hPS and hPB.

Fast Stirring. In a second bulk run, a high-speed propeller stirrer was used, at 1500 rpm. This changed the kinetics drastically. The vigorous stirring activated the grafting to a degree that the demixed bulk system yielded practically the same balance of homopolymer and graft copolymer formation as in homogeneous solution. (In industries, where the reactors and stirrers

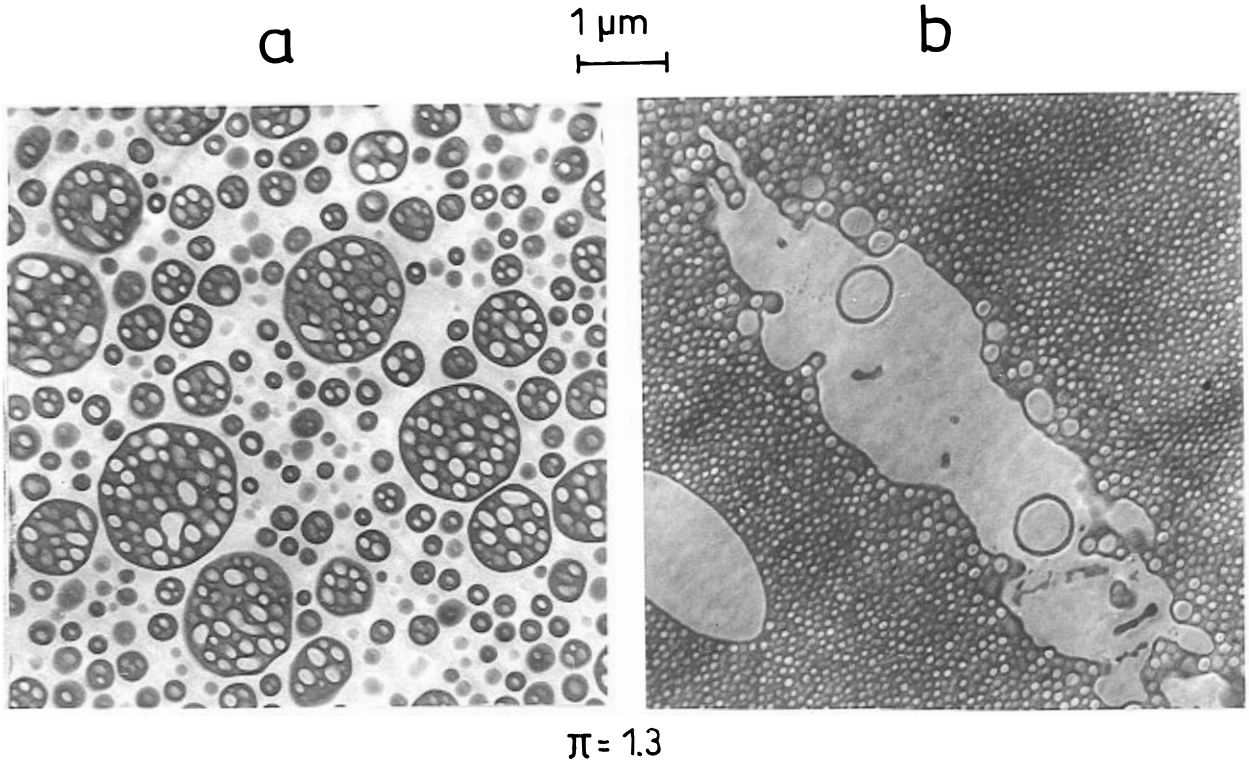

Figure 14. Bulk polymerization, fast stirring: (a) in situ and (b) cast-film morphology at intermediate conversion ($\pi = 1.3$). Matrix: hPS in (a), hPB in (b).

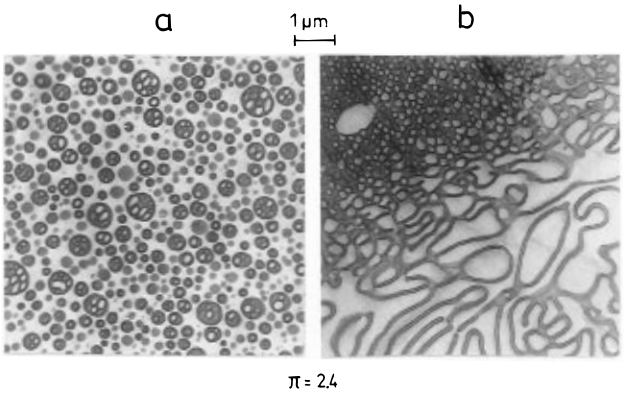

Figure 15. Bulk polymerization, fast stirring: (a) in situ and (b) cast-film morphology at high conversion ($\pi = 2.4$). Macrophase−microphase transition in (b).

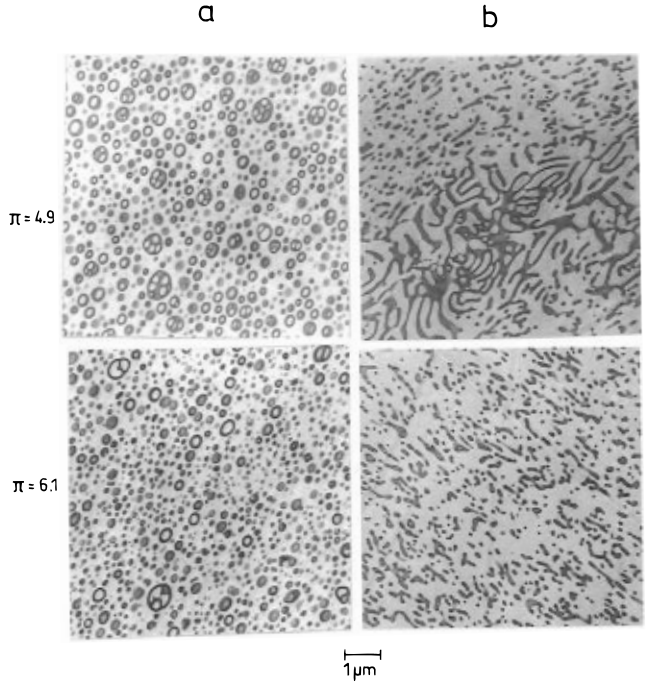

Figure 16. Bulk polymerization, fast stirring: (a) in situ and (b) cast-film morphology at very high conversion ($\pi = 4.9$ and $\pi = 6.1$). Almost micellar structures.

are built more efficiently, this balance is achieved even at much lower stirrer speeds than used in this study.)

The hPS/hPB/PBgS blends were isolated from samples taken from the rapidly stirred polymerizing bulk system via two routes: (i) directly, by evaporation of the styrene ("in situ"), and (ii) indirectly, by dilution with toluene, precipitation, and redissolution in toluene, followed by slow film casting ("cast film"). The morphologies of blends i are shown in Figures 13a−16a; those of blends ii, in Figures 13b−16b. The structures are strikingly different.

Route i of styrene evaporation was used to isolate the hPS/hPB/PBgS blends with the unchanged *in-situ morphology* of the polymerizing hPS/hPB/PGgS/styrene system. Except perhaps at low conversion (Figure 13a), where much styrene had to be evaporated off, this worked amazingly well: The phase structures in Figures 14a−16a should be quite exactly the original morphologies. Complex domain structures as in Figure 14a should not undergo major changes during styrene evaporation, particularly as the system is already rather viscous.

The expected matrix inversion (Figure 3b) occurs between $\pi = 0.4$ (Figure 13a) and $\pi = 1.3$ (Figure 14a). It probably takes place in the range of $\pi = 1$, from where on hPS is the matrix. Characteristic HIPS structures with their salami domains of hPB/PBgS appear right after the matrix inversion, in Figures 14a and 15a. At even higher π, the salami domains disintegrate successively to the stage of micelles (Figure 16a).

To interpret these structures, it is informative to compare the morphologies in Figures 13a−15a with the cast-film morphologies in Figure 13b−15b. [As in Figures 9 and 10, the orientation of the structure in the cast-film pictures is disregarded as an artifact of film casting.]

Route ii of film casting was used to accomplish the opposite to route i: Precipitation of a hPS/hPB/PBgS blend and redissolution in toluene erase all memory of the in-situ structures in the polymerizing system. During subsequent film casting, the blend components can arrange according to their mutual compatibility. If a nonselective solvent as, in this system, toluene, is used, the cast film exhibits a *thermodynamically controlled blend morphology*.[27]

The cast-film morphologies in Figures 13b−15b do not look at all like the in-situ morphologies in Figures 13a−15a. Instead, they look like the cast-film morphologies in Figures 9 and 10, showing the same transition stages and fractionation effects: The kinetics of the styrene polymerization are surprisingly similar in a homogeneous PB/styrene/toluene solution and in a demixed, but rapidly stirred, bulk PB/styrene mixture. (Note that Figures 13−15 have a higher magnification than Figures 9 and 10.)

The close similarity of the solution run and the bulk run is confirmed by Figure 16b. It shows the bulk run at high conversions π that were not analyzed in solution. Yet, the microstructures in Figure 16b could have been readily predicted by extrapolation from Figure 10b: Inverse-cylindrical and inverse-spherical micelles ($G >$ 2 behavior) dominate.

Particularly informative are Figure 14a,b. The two structures look very different, but they are, in fact, *matrix-inverted twins*. The cast-film morphology of the hPS/hPB/PBgS blend in Figure 14b indicates that the process is approximately in the stage of the solution system in Figure 9b. In this stage, hPB forms the matrix phase. It is filled with micelles of copolymer chains of the type PBgS(G=1). The homopolymer hPS forms macrodomains, the irregular surface of which is stabilized by a layer of copolymer chains of the type PBgS($G\geq 2$). These PBgS($G\geq 2$) copolymers form also two closed lamellar circles inside the hPS domain in Figure 14b.

Figure 14b explains Figure 14a, too: The characteristic HIPS macrodomains in Figure 14a must be stabilized on the outside by copolymer chains of the type PBgS($G\geq 2$) while the subdomains on the inside are micelles of copolymer chains of the type PBgS(G=1).

At higher π, the fraction of PBgS($G\geq 2$) copolymer chains grows at the expense of PBgS(G=1) copolymer chains and of the hPB homopolymer chains. This leads in Figures 15a and 16a to domain structures with an increased outer surface and a decreased inner surface: The macrodomains disintegrate until only micelles are left, made of copolymer chains of the type PBgS($G\geq 3$). In these late stages, the in-situ and the cast-film morphologies are similar. The system has nearly reached the micellar stage in Figure 16a, at $\pi = 6.1$, where half of the styrene is polymerized.

A final note is added here concerning cast films, since they are important for the above conclusions. Film casting was considered in all generality in ref 27. The summary is that the size and shape of macrodomains in film morphologies depend sensitively on details of the casting and should not be discussed. Important is the arrangement of the phases, i.e. the question of which phases touch or solubilize each other. In films cast from nonselective solvents, these arrangements are established as prescribed by thermodynamics: The favored arrangement of all phases is observed. This thermodynamic control is pivotal for the above discussion.

6. Discussion

The factors controlling the HIPS process have been known for many years, but the exact mechanism leading to the unique salami morphologies (Figure 1) has remained uncertain. The data of this study, notably the cast-film morphologies in Figures 9 and 10 and Figures 13b−16b and the in-situ morphologies in Figures 13a−16a, suggest the following conclusions:

(i) Kinetics. The styrene polymerization in homogeneous PB/styrene/toluene solutions and in rapidly stirred bulk PB/styrene mixtures is similar. The kinetics are straightforward. Thus the HIPS morphology is not caused by extraoridinary kinetics of the homopolymerization and the graft copolymerization.

(ii) Compatibility of the Copolymer and the Homopolymers. It is often taken for granted that the graft copolymer PBgS acts, in the hPS/hPB/PBgS/styrene system, as a "compatibilizer". If so, the copolymer should concentrate between the phases of the homopolymers, the gPS grafts mixing with hPS and the gPB backbones with hPB, thereby subdividing these phases down to submicroscopic structures, as seen in Figure 10b and 15b. But only the chains PBgS($G\geq 2$) with more than one gPS graft, which are created fairly late at high π are compatibilizers in this sense. The PBgS(G=1) chains that are created first, at low π, carry only one gPS graft which is, moreover, much shorter than the gPB backbone. This single graft does not mix with long-chained hPS (Figures 9, 13b, and 14b), so that the PBgS(G=1) copolymer chains are not compatibilizers. They exclusively form micelles within the hPB phase.

(iii) Matrix Inversion. The homopolymer hPS takes over the matrix in the range of $\pi = 1$ (Figures 13a and 14a). This seems natural, at first glance, since $\pi = 1$ means equal amounts of PS (i.e. hPS + gPS) and PB (i.e. hPB + gPB). Yet the point of matrix inversion, if thermodynamically controlled, i.e. if driven by the surface tension, occurs not at equal weights of the components, but at equal weights (more exactly, volumes) of the coexisting phases.

In the range $\pi = 1$, a major phase of hPB/PBgS(G=1) coexists with a minor phase of hPS. The matrix inversion is expected at a higher conversion π where

$$(w_{\mathrm{hPB}} + w_{\mathrm{PBgS}})(\pi)/w_{\mathrm{hPS}}(\pi) = 1 \qquad (14)$$

According to Figure 5c and eq 12, this happens approximately at $\pi = 2$. This means that the matrix should be hPB up to $\pi = 2$. Indeed, this is the case in the thermodynamically controlled cast-film morphologies of Figures 9 and 10a and Figures 13b and 14b ($\pi <$ 2).

But the in-situ morphology in Figure 13a exhibits at $\pi = 1.3$ already all characteristic features of HIPS. In particular, it has a matrix of hPS. This early matrix inversion during the HIPS process *cannot be explained thermodynamically*. It is rheologically based.

(iv) Domain Structure. With points ii and iii, the particular salami structure of HIPS can be understood: The early matrix inversion produces the salami morphology at a stage (Figure 14a) where most graft

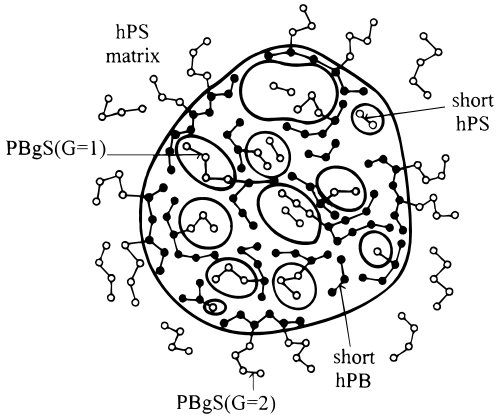

Figure 17. Molecular interpretation of the salami domains in Figure 14a.

copolymer chains are still of the type PBgS(G=1). These PBgS(G=1) copolymer chains, unable to solubilize hPS, provide the micellar subdomains inside the salami domains. A small share of the copolymer chains of the type PBgS(G=2) covers these domains on the outside and stabilizes their surface.

Ongoing grafting and stirring at higher π disintegrate the salami domains until only micelles are left (Figure 16a).

This disintegration due to "overgrafting" must be avoided in industries, since micelles to not improve the impact resistance of PS efficiently. The salami domains in Figure 14a or 15a are, therefore, preserved by slowing down the grafting at higher π. During the polymerization step 2 → 3 indicated in Figure 3b, the vigorous stirring is discontinued and transfer agents are added, so that mainly hPS is produced.

The main conclusion from this study, concerning the characteristic HIPS structures in Figure 14a (and Figure 15a), is that the *salami domains are hPB domains, heavily filled by PBgS(G=1) micelles and surrounded by a PBgS(G=2) surface layer*, as indicated in Figure 17. Approximately, this describes also the domains in the commercial HIPS shown in Figure 1. But the picture must be modified a bit. An explanation is needed for the very large subdomains inside the salami domains in Figure 1. These subdomains are not simple micelles, but micelles filled with hPS. There are some slightly filled micelles inside the domains in Figure 14a, too, but the swelling is in some domains in Figure 1 much stronger.

The difference is that Figure 14a shows the salami domains practically at birth, i.e. just after the phase inversion, while Figure 1 shows an end product. The former stage corresponds to point 2 in Figure 3b and the final stage to point 3. As mentioned above, step 2 → 3 is carried out, in industries, under conditions that subdue the grafting and preserve the salami structure. However, some grafting goes on in this step 2 → 3, which produces some PBgS(G>1) chains even inside the salami domains. This permits some micelles to take up hPS and to swell. In conclusion, an appropriate description of commercial HIPS morphologies should be that the domains contain micelles of PBgS($G \leq 2$), more or less filled with (probably short-chained) hPS, and are covered by a skin of PBgS($G \geq 2$).

Acknowledgment. Financial support from the EEC through a Brite-Euram research project (4260-90) is gratefully acknowledged. We would like to thank Dr. K. Knoll and Dr. W. Loth (BASF AG) for helpful discussions and Dr. F. Gruber (BASF AG) for the triblock copolymer in Figure 2b.

Appendix

Several authors have analyzed the kinetics of styrene grafting in PB/styrene mixtures.[19,20,22,28] The following equations disregard minor side reactions and are, therefore, comparatively straightforward. The background of the equations in the theoretical section is indicated.

Equation 3. Simple kinetics of radical polymerization yield eq 3 for the conversion π, with the familiar rate constant

$$k = \sqrt{R_i}(k_p/\sqrt{k_t})$$

R_i = rate of initiator decay; k_p, k_t = rate constants of chain propagation and termination (A1)

Equation 4. The production of hPS, related to that of all PS, is

$$(dm_{hPS}/dm_{PS})(t) = ([hPS^\bullet]^2 + [hPS^\bullet][gPS^\bullet])/([hPS^\bullet] + [gPS^\bullet])^2(t) = 1/(1 + C/(R - \pi(t))) \quad (A2)$$

where the second relation is derived from the ratio of the stationary radical concentrations

$$[gPS^\bullet]/[hPS^\bullet] = C/(R - \pi) \quad (A3)$$

Integration leads to

$$f_{hPS} = (1/\pi)\int d\pi/(1 + C/(R - \pi)) = 1 + (C/\pi)\ln(1 - \pi/(R + C)) \quad (A4)$$

which yields, at the values of R, C, and π of this paper, eq 4. Equation A3 is subject to the assumption of chain termination by radical disproportionation. In reality, the polymerization of styrene in toluene involves also combination and transfer to the solvent. The first increases and the second decreases the chain lengths. Therefore, assuming disproportionation seems a fair compromise.

Equations 6−10. The combined analysis of the chains of hPB and PBgS is based on three probability parameters, β, σ, and γ, i.e. the two probabilities that a butadiene unit (β) or a styrene unit (σ) is a chain end and the probability that a butadiene unit is a graft point (γ). The first two are given by the inverse (number average) degrees of polymerization

$$\beta = 1/P_{PB} \qquad \sigma = 1/P_{PS} \quad (A5)$$

and the last by

$$\gamma = (1 - f_{hPS})\pi(M_B/M_S)\sigma \quad (A6)$$

Only γ changes with the conversion π, while β and σ are constant. P_{PB}, P_{PS}, and π are primary observables, and only f_{hPS} is itself a derived parameter (eq A4).

The probability distribution of PB chains having b units and g grafts is given by $n_b n_g$ where the separate probabilities are

$$n_b = (\beta/(1 - \beta))(1 - \beta)^b$$

$$n_g = \binom{b}{g}(\gamma/(1 - \gamma))^g(1 - \gamma)^b \quad (A7)$$

Equations 6 and 7. If all PB chains are considered together, hPB and PBgS, the (number average) number of grafts per PB chain is

$$G^* = \gamma/\beta \tag{A8}$$

which is intuitively obvious. If hPB is excluded and only PBgS is considered, the number of grafts per gPB chain is

$$G = (1/\beta)(1 - (1 - \beta)(1 - \gamma)) \tag{A9}$$

of which eq 6 is a good approximation.

Equations 8−10. The probability distribution of hPB chains having b butadiene units is (eq A7)

$$n_b n_{g=0} = (\beta/(1 - \beta))((1 - \beta)(1 - \gamma))^b \tag{A10}$$

This leads to the fraction of the ungrafted homopolymer hPB

$$f_{\mathrm{hPB}} = \sum b n_b n_{g=0} / \sum b n_b = (1 - \gamma)\beta^2/(1 - (1 - \beta)(1 - \gamma))^2 \tag{A11}$$

of which eq 8 is a good approximation, and to the degree of polymerization

$$P_{\mathrm{hPB}} = \sum b n_b n_{g=0} / \sum n_b n_{g=0} = 1/(1 - (1 - \beta)(1 - \gamma)) = P_{\mathrm{PB}}/G \tag{A12}$$

This means that the ungrafted hPB chains are just as long as the distance between two grafts in the gPB subchains of the corresponding graft copolymer PBgS.

The probability distribution of gPB subchains of the copolymer PBgS having b butadiene units is $n_b(1 - n_{g=0})$ (eqs A7 and A10) and the degree of polymerization is given by

$$P_{\mathrm{gPB}} = (1/\beta)(1 - (1 - \beta)^2(1 - \gamma))/(1 - (1 - \beta)(1 - \gamma)) \tag{A13}$$

which yields the good approximation eq 10.

Equation 11. The probability distribution of hPS chains having s styrene units is

$$n_s = (\sigma/(1 - \sigma))(1 - \sigma)^s \tag{A14}$$

The gPS grafts in the PBgS copolymer chains have the same distribution. However, more important for the description of the PBgS chains is not the length of a single graft, but that of all grafts in one PBgS chain. The probability distribution of g gPS grafts having, together, s styrene units is the $(g - 1)$-fold convolution of eq A13

$$n_{gs} = \binom{s-1}{g-1}(\sigma/(1 - \sigma))^g(1 - \sigma)^s \tag{A15}$$

The combined probability distribution of PBgS chains having b butadiene units and s styrene units in g grafts is $n_b n_g n_{gs}$ (eqs A7 and A15). Since two monomer units are involved in PBgS, it is useless to calculate degrees of polymerization. The (number average) molecular weight is given by

$$M_{\mathrm{PBgS}} = \sum (bM_{\mathrm{B}} + sM_{\mathrm{S}}) n_b n_g n_{gs} / \sum n_b n_g n_{gs} \tag{A16}$$

which yields, in fact, simple equations. The result is

$$M_{\mathrm{PBgS}} = (M_{\mathrm{PB}} + G^* M_{\mathrm{PS}}) \tag{A17}$$

if hPB and PBgS are described together, and eq 11, if only PBgS is described.

References and Notes

(1) Echte, A.; Haaf, F.; Hambrecht, J. *Angew. Makromol. Chem.* **1981**, *93*, 372.
(2) Echte, A. In *Chemische Technologie*, 4th ed.; Winnaker, Küchler, Eds.; Hanser: Munich, 1981; Chapter 4.2.2.3, p 381.
(3) Platt, A. E.; Wallace, T. C. In *Kirk-Othmer Encyclopedia of Chemical Technology*, 3rd ed.; Grayson, M., Ed.; Wiley Interscience: New York, 1983; Vol. 21, p 822.
(4) Riess, G.; Gaillard, P. In *Polymer Reaction Engineering—Influence of Reaction Engineering on Polymer Properties*; Reichert, K. H., Geiseler, W., Eds.; Hanser: Munich, 1983; p 221.
(5) Wagner, E. R.; Robeson, L. M. *Rubber Chem. Technol.* **1970**, *43*, 1129.
(6) Echte, A. *Angew. Makromol. Chem.* **1977**, *58/59*, 175; *Adv. Chem. Ser.* **1989**, *222*, 15.
(7) Retting, W. *Agnew. Makromol. Chem.* **1977**, *58/59*, 133.
(8) Bucknall, C. B. *Toughened Plastics*; Applied Science Publishers: London, 1979; *Makromol. Chem., Macromol. Symp.* **1988**, *20/21*, 425.
(9) Michler, G. H. *Kunststoff-Mikromechanik*; Hanser: Munich, 1992; p 241.
(10) McMaster, L. P. *Adv. Chem. Ser.* **1975**, *142*, 43.
(11) Andradi, L. N.; Hellmann, G. P. *Polymer* **1993**, *34*, 925; *Polym. Eng. Sci.* **1994**, *35*, 693.
(12) Inoue, T.; Soen, T.; Hashimoto, T.; Kawai, H. *Macromolecules* **1970**, *3*, 87; In *Block Copolymers*; Aggarwal, S. L., Ed.; Plenum: New York, 1970; p 53.
(13) Aggarwal, S. L. *Polymer* **1976**, *17*, 938.
(14) Löwenhaupt, B.; Hellmann, G. P. *Polymer* **1991**, *32*, 1065.
(15) Löwenhaupt, B.; Steurer, A.; Hellmann, G. P.; Gallot, Y. *Macromolecules* **1994**, *27*, 908.
(16) Eastmond, C.; Phillips, D. G. *Polymer* **1979**, *20*, 1501.
(17) Jiang, M.; Huang, X.; Yu, T. *Polymer* **1983**, *24*, 1259.
(18) Braun, D.; Fischer, M.; Hellmann, G. P. *Makromol. Chem., Macromol. Symp.* **1994**, *83*, 77.
(19) Brydon, A.; Burnett, G. M.; Cameron, G. G. *J. Polym. Sci., Polym.* 4Chem. **1973**, *11*, 3255; **1974**, *12*, 1011.
(20) Fischer, J. P. *Angew. Makromol. Chem.* **1973**, *33*, 35.
(21) Kruse, R. L. *Adv. Chem. Ser.* **1975**, *142*, 141.
(22) Ludwico, W. A.; Rosen, S. L. *J. Polym. Sci., Polym. Chem.* **1976**, *14*, 2121.
(23) Rigler, J. K.; Müller, L.; Wolf, B. A. *Angew. Makromol. Chem.* **1978**, *74*, 113.
(24) Molau, E. *J. Polym. Sci., Part A: Polym. Chem.* **1965**, *3*, 1267, 4235.
(25) Molau, E.; Keskkula, H. *J. Polym. Sci., Polym. Chem. Ed.* **1966**, *4*, 1595.
(26) Keskkula, H. *Plast. Rubber Mater. Appl.* **1979**, *4*, 66, 71.
(27) Yu, D.; Andradi, L. N.; Hellmann, G. P. *Makromol. Chem.* **1991**, *192*, 2615.
(28) Tung, L. H.; Wiley, R. M. *J. Polym. Sci., Polym. Phys.* **1973**, *11*, 1413.

MA950779A